Green's Function Based Simulation of the Optical Spectrum of Multisection Lasers

Hans Wenzel

***Abstract*—A new approach for the calculation of the optical spectrum of semiconductor lasers is presented. It is based on a solution of the inhomogeneous coupled wave equations using the Green's function method. The spontaneous emission is modeled by Langevin noise functions. In contrast to previous theories, lasers with gain-coupled distributed feedback sections are properly described. The theoretical model is used in a fitting procedure for parameter extraction.**

***Index Terms*—Amplified spontaneous emission, distributed feedback (DFB) laser, Green's function method.**

I. Introduction

THE SPECTRUM of the amplified spontaneous emission (ASE), measured at the facets of semiconductor lasers below threshold, contains important information about fundamental laser parameters that are difficult to access otherwise. Among these parameters are those which describe the properties of the semiconductor active medium such as the optical gain [1] and the refractive index, as well as those that are closely related to the optical cavity itself such as the reflectivities of the facets, parasitic reflections within the cavity [2], and coupling coefficients of Bragg gratings in distributed feedback (DFB) lasers.

To our knowledge, a first calculation of the ASE of index-coupled DFB lasers was performed by Soda and Imai [3]. They used the standard procedure of summing up an infinite number of reflections of radiation originating at position z into a convergent geometric series to obtain the emitted radiation. Later, this method was adapted and improved by many others; cf. [4]–[7], and [8]. The disadvantage of this approach is that continuously varying refractive indexes and other parameters can only be treated if the cavity is subdivided into a number of sections where all parameters are set constant. Additionally, the spectral shape of the local spontaneous emission is mostly neglected.

Another popular method was introduced by Henry [9]. He treated spontaneous emission as a Langevin function noise term in the wave equation and solved the resulting inhomogeneous equation by calculating its Green's function in terms of the Wronskian of the homogeneous equation. This method was used in [10]–[12], too. The disadvantage of this method is the need to calculate the Wronskian of the wave equation.

Schatz *et al.* calculated the Green's function directly, which resulted in a rather simple expression for the ASE spectrum of single-section DFB lasers [13]. Further models are based on 3×3 transfer matrices [14], classical electrical network theory [15], and spontaneous emission current sheets [16].

In addition to the different approaches to treat the spontaneous emission, there are essentially two methods to solve the wave equation for the calculation of the ASE. One method is to solve the wave equation directly by means of transfer matrices [5], [8], and the other one is to convert the second-order differential equation into two first-order equations for the amplitudes of the forward- and backward-propagating waves by an averaging procedure [17]. For DFB lasers, both equations are coupled by the so-called coupling coefficient. Some authors using the transfer-matrix method regard the coupled wave equations to be less accurate. However, detailed investigations have shown that both methods are equivalent as far as certain conditions are fulfilled [17], [18]. The advantage of the coupled wave equations is that a DFB laser containing thousands of high- and low-index regions can be discretized in much larger steps.

If the laser parameters the ASE spectrum depends on are treated as unknown variables in the theoretical models, it is possible to determine them by comparing calculated and measured spectra. This has been demonstrated in [6], [7], [19], and [20]. For single-section DFB lasers, a commercial [21] as well as a free [22] computer program for parameter extraction is now available.

Despite this success, there is still a controversy about the correct model of the ASE to be used, especially for gain-coupled DFB lasers. In [8], it was claimed that from a quantum-mechanical point of view, an interference term between forward- and backward-propagating spontaneously emitted photons should appear in the expression for the ASE, and that this term is absent in all references except [14]. Actually, the interference term is included in the Green's function method described in [9] and the papers based on this article, as it was later corrected by Morrison and Cassidy [23]. However, the interference term has not so far been included in most of the calculations of the ASE below threshold and, nevertheless, a good agreement with measurements was found. Therefore, the question arises whether this term is important or not.

The aim of this paper is the derivation of a new Green's function based solution of the inhomogeneous coupled wave equations. Spontaneous emission is introduced by Langevin noise functions. The laser cavity may consist of an arbitrary number of active and passive sections with and without Bragg gratings. The theoretical model is consistent with the well-established theory for the spectral linewidth, the sidemode suppression ratio, and other noise properties of the lasing mode of multisection lasers including gain-coupled DFB lasers; cf. [24], [25] and [26] and the references therein. The theoretical model is used in a parameter extraction program and its applicability is demonstrated for a few examples.

Manuscript received December 13, 2002; revised June 12, 2003.

The author is with the Ferdinand-Braun-Institut für Höchstfrequenztechnik, 12489 Berlin, Germany (e-mail: wenzel@fbh-berlin.de).

Digital Object Identifier 10.1109/JSTQE.2003.818344

II. Theoretical Model

A. Basic Equations

Our aim is to calculate the spontaneously emitted optical field propagating along the axis (z) of a one-dimensional multisectional cavity filled at least partially with a semiconductor active medium. We assume that in the transverse (x,y) plane only a single guided mode exists, and that only the longitudinally varying part is time-dependent. The time-dependence is expressed via a Fourier integral. Hence, the main transverse electric and magnetic field components are given by

$$E(x,y,z,t) = \frac{A(x,y)}{\sqrt{2\pi}} \int_{-\infty}^{+\infty} E_\omega(z) \mathrm{e}^{i\omega t}\, d\omega$$
$$H(x,y,z,t) = \frac{B(x,y)}{\sqrt{2\pi}} \int_{-\infty}^{+\infty} H_\omega(z) \mathrm{e}^{i\omega t}\, d\omega \qquad (1)$$

where for TE-like modes, for example, $E \equiv E_y$ and $H \equiv H_x$ hold. The transverse field functions (mode distributions) $A(x,y)$ and $B(x,y)$, which may depend parametrically on the longitudinal coordinate z, are normalized according to

$$\frac{1}{2} \iint \mathrm{Re}\{A(x,y)B^*(x,y)\}\, dx\, dy = \mp 1 \qquad (2)$$

where $*$ denotes the complex conjugate and the upper (lower) sign holds for TE (TM) modes. The Fourier components are decomposed into waves propagating forward and backward along the longitudinal laser axis

$$E_\omega(z) = \psi_\omega^+(z)\mathrm{e}^{-i\beta_0 z} + \psi_\omega^-(z)\mathrm{e}^{+i\beta_0 z}$$
$$H_\omega(z) = \psi_\omega^+(z)\mathrm{e}^{-i\beta_0 z} - \psi_\omega^-(z)\mathrm{e}^{+i\beta_0 z}. \qquad (3)$$

Here, β_0 is a real valued reference propagation factor. For DFB sections, for example, it is given by $m\pi/\Lambda$, where m is the order and Λ the period of the Bragg grating. The slowly varying amplitudes of the forward- and backward-propagating waves ψ_ω^+ and ψ_ω^-, respectively, obey the so-called coupled wave equations [17], [18], [27]

$$\mathbf{H}_\omega(z)\Psi_\omega(z) = \mathrm{F}_\omega(z) \qquad (4)$$

where we introduced the vector notation

$$\Psi_\omega = \begin{bmatrix} \psi_\omega^+ \\ \psi_\omega^- \end{bmatrix}. \qquad (5)$$

The term

$$\mathrm{F}_\omega = \begin{bmatrix} f_\omega^+ \\ f_\omega^- \end{bmatrix} \qquad (6)$$

on the right-hand side of (4) consists of Langevin noise functions, which model the randomly distributed spontaneous emission events. Details are presented in Section II-B.

The matrix operator in (4) reads

$$\mathbf{H}_\omega = \begin{bmatrix} +\frac{\partial}{\partial z} + i\Delta\beta - \kappa_i^{\mathrm{rad}} & i\kappa^+ \\ i\kappa^- & -\frac{\partial}{\partial z} + i\Delta\beta - \kappa_i^{\mathrm{rad}} \end{bmatrix} \qquad (7)$$

where $\Delta\beta(\omega,z) = \beta(\omega,z) - \beta_0$ is the relative propagation coefficient. The imaginary part can be written as

$$\mathrm{Im}\Delta\beta(\omega,z) \equiv \mathrm{Im}\beta(\omega,z) = \frac{1}{2}[g(\omega,z) - \alpha(\omega,z)] \qquad (8)$$

where g is the modal gain and α the modal loss coefficient, both averaged over one grating period.

The coupling coefficients are complex valued. The real and imaginary parts may depend additionally on a common phase

$$\kappa^\pm(z) = [\kappa_\mathrm{r}(z) + i\kappa_\mathrm{i}(z)]\mathrm{e}^{\mp 2\pi i\varphi(z)}. \qquad (9)$$

In this way, index, gain, and absorption coupled DFB sections with first or higher order Bragg gratings can be accounted for. Note that the signs of the real and imaginary parts of $\kappa^\pm, \kappa_r$, and κ_i, respectively, have to be chosen properly. For example, in the case of an antiphase gain grating, $\kappa_i < 0$ must be ensured if $\kappa_r > 0$ has been chosen. For a second-order index grating, $\kappa_i = \kappa_i^{\mathrm{rad}} < 0$ holds, and the sign of κ_r depends on the duty cycle of the grating [28]. The phase φ allows a modeling of phase-shifted gratings. For a second-order grating (and similarly for higher- order gratings), the imaginary part of the coupling coefficient κ_i^{rad} due to first-order radiation has to be added to the relative propagation coefficient[1] [28].

At the facets of the laser, we assume the usual reflecting boundary conditions for the propagating wave amplitudes

$$\psi_\omega^+(0) - r_0\psi_\omega^-(0) = 0 \qquad (10)$$
$$\psi_\omega^-(L) - r_L\psi_\omega^+(L) = 0. \qquad (11)$$

At an interface between two sections located at $z = z_d$, the following most general transition condition for the amplitudes on both sides of the interface is assumed to be valid:

$$\begin{bmatrix} \psi_\omega^+(z_d^>) \\ \psi_\omega^-(z_d^>) \end{bmatrix} = \frac{1}{t^-} \begin{bmatrix} t^+t^- - r^+r^- & r^- \\ -r^+ & 1 \end{bmatrix} \begin{bmatrix} \psi_\omega^+(z_d^<) \\ \psi_\omega^-(z_d^<) \end{bmatrix}. \qquad (12)$$

If there is no scattering loss or absorption at the interface, the energy conservation condition requires $t^+t^- - r^+r^- = 1$ and $r^- = -r^{+*}$.

B. Langevin Noise Functions

The ensemble averages of the Langevin noise functions vanish

$$\langle f_\omega^\pm(z)\rangle = 0 \qquad (13)$$

and the correlation functions are given by [24] and [27]

$$\langle f_\omega^+(z) f_{\omega'}^{+*}(z')\rangle = \langle f_\omega^-(z) f_{\omega'}^{-*}(z')\rangle = 2D_\omega(z)\delta(z-z')\delta(\omega-\omega'). \qquad (14)$$

All other combinations of $f_\omega^\pm$ and their complex conjugates can be assumed to be uncorrelated, except for gain-coupled DFB sections where additionally

$$\langle f_\omega^+(z) f_{\omega'}^{-*}(z')\rangle = 2D_\omega^{\mathrm{gc}}(z)\delta(z-z')\delta(\omega-\omega') \qquad (15)$$

together with its complex conjugate holds. The reason for the fact, that except for gain-coupled DFB sections the cross correlation between the Langevin noise functions for the forward- and backward-propagating waves can be neglected within the coupled wave formalism is the rapidly oscillating term $\mathrm{e}^{+2\beta_0 z}$ appearing in the calculation of the correlation functions between f_ω^+ and f_ω^{-*} (compare [29]). However, in gain-coupled DFB sections, the modal gain before averaging $g + 4\kappa_i^{\mathrm{gc}}\cos(2\beta_0 z +$

[1]Identical only for gratings with inversion symmetry.

$2\pi\varphi$) is spatially modulated by the same period that leads to a cancellation of the rapidly oscillating term.

According to [24] and [27], the diffusion coefficients are given by

$$2D_\omega(z) = \hbar\omega g(\omega, z) n_{\rm sp}(\omega, z) \tag{16}$$

and

$$2D_\omega^{\rm gc}(z) = 2\hbar\omega\kappa_i^{\rm gc}(\omega, z)\mathrm{e}^{-2\pi i\varphi} n_{\rm sp}(\omega, z). \tag{17}$$

In (16) and (17), $n_{\rm sp}$ is the spontaneous emission factor, $\hbar$ Planck's constant divided by 2π, $\kappa_i^{\rm gc}$ the imaginary part of the coupling coefficient of a gain grating. For gain-guided lasers, the diffusion coefficients have to be multiplied with Petermann's spontaneous emission enhancement factor K [30].

C. Solution

For the following, we define the inner product

$$(\Psi_\omega(z), \Phi_\omega(z)) = \int_0^L [\psi_\omega^+(z)\phi_\omega^-(z) + \psi_\omega^-(z)\phi_\omega^+(z)]\, dz. \tag{18}$$

The operator $\mathbf{H}_\omega$ is symmetric [31], i.e., within the product (18) it can be interchanged, so that

$$(\Psi_\omega(z), \mathbf{H}_\omega(z)\Phi_\omega(z)) = (\mathbf{H}_\omega(z)\Psi_\omega(z), \Phi_\omega(z)) \tag{19}$$

holds for any two-component functions Ψ_ω and Φ_ω that obey the boundary conditions (10) and (11). Using this inner product (18), we can write the solution of (4) as

$$\Psi_\omega(z) = \begin{bmatrix} (\mathrm{G}_{1,\omega}(z, z'), \mathrm{F}_\omega(z')) \\ (\mathrm{G}_{2,\omega}(z, z'), \mathrm{F}_\omega(z')) \end{bmatrix} \tag{20}$$

where the Green's functions

$$\mathrm{G}_{1,\omega}(z, z') = \begin{bmatrix} g_{1,\omega}^+(z, z') \\ g_{1,\omega}^-(z, z') \end{bmatrix} \tag{21}$$

and

$$\mathrm{G}_{2,\omega}(z, z') = \begin{bmatrix} g_{2,\omega}^+(z, z') \\ g_{2,\omega}^-(z, z') \end{bmatrix} \tag{22}$$

obey the following inhomogeneous coupled wave equations with Dirac's δ-function as source term

$$\mathbf{H}_\omega(z)\mathrm{G}_{1,\omega}(z, z') = \begin{bmatrix} 0 \\ \delta(z - z') \end{bmatrix} \tag{23}$$

$$\mathbf{H}_\omega(z)\mathrm{G}_{2,\omega}(z, z') = \begin{bmatrix} \delta(z - z') \\ 0 \end{bmatrix} \tag{24}$$

subject to the same boundary conditions (10) and (11) (for both arguments) as satisfied by Ψ_ω. The proof that (20) solves (4) is given in Appendix A.

D. Calculation of Optical Spectrum

Taking into account the normalization (2), the power spectral density of the forward- and backward-propagating waves is given by [9], [32]

$$S_\omega^\pm(z) = \int_{-\infty}^{+\infty} \langle \psi^\pm(z, t)\psi^{\pm *}(z, 0)\rangle \mathrm{e}^{-i\omega t}\, dt \tag{25}$$

where

$$\psi^\pm(z, t) = \frac{1}{\sqrt{2\pi}} \int_{-\infty}^{+\infty} \psi_\omega^\pm(z)\mathrm{e}^{i\omega t}\, d\omega. \tag{26}$$

Introducing (26) into (25) yields

$$S_\omega^\pm(z) = \int_{-\infty}^{+\infty} \langle \psi_\omega^\pm(z)\psi_{\omega'}^{\pm *}(z)\rangle\, d\omega'. \tag{27}$$

To this end, the power spectral density can be evaluated with the help of the solution (20) of the coupled wave equations with Langevin noise sources, taking into account the correlation functions (14) and (15). Here, we are interested in the ASE emerging from the left facet $z = -0$, which can be expressed as

$$\begin{aligned} S_\omega^-(-0) = (1 - |r_0|^2) & \\ \times \Bigg\{ & \int_0^L [|g_{2,\omega}^+(0, z)|^2 + |g_{2,\omega}^-(0, z)|^2] 2D_\omega(z)\, dz \\ & + 2\int_0^L \mathrm{Re}\{g_{2,\omega}^{+*}(0, z) g_{2,\omega}^-(0, z) 2D_\omega^{\rm gc}(z)\}\, dz \Bigg\}. \end{aligned} \tag{28}$$

Equation (28) represents the main result of this paper. It consists of two terms. The first term corresponds to what is obtained, for example, by the multireflection method [3] or the Green's function method for the wave equation [10] neglecting the interference between forward- and backward-propagating spontaneously emitted photons. The second term arises from the cross correlation (15) present only for gain-coupled DFB sections. For Fabry–Perot (FP) as well as index and absorption coupled DFB sections, within the coupled wave formalism there is no interference term for the reasons discussed above. This finding is in agreement with [8] where, although the importance of the interference term was pointed out, it was found that this term only has an impact on the spectra of gain-coupled DFB lasers. The interference term has its analog in a corresponding term in the stimulated recombination rate (standing wave effect [27]).

It should be mentioned that (28) holds only as far as the stimulated recombination can be omitted so that the carrier fluctuations have no influence on the photon fluctuations, i.e., below threshold or beyond the lasing mode above threshold.

It is instructive to compare (28) with the corresponding expression derived in [33], (60) on the basis of a quantum mechanical nonequilibrium Green's function technique for the photons and the carriers. The polarization function $P^<(\omega)$ in [33] is proportional to D_ω and the retarded Green's function there is closely related to $\mathrm{G}_{1,\omega}$ and $\mathrm{G}_{2,\omega}$.

To close this section, we show in the following how the Green's function $\mathrm{G}_{2,\omega}(0, z) = \mathrm{G}_{2,\omega}(z, 0)$ can be calculated efficiently. It solves the homogeneous coupled wave equation

$$\mathbf{H}_\omega(z)\mathrm{G}_{2,\omega}(z, 0) = 0 \tag{29}$$

subject to an inhomogeneous boundary condition at $z = 0$

$$g_{2,\omega}^+(0, 0) - r_0 g_{2,\omega}^-(0, 0) = 1. \tag{30}$$

At $z = L$, the homogeneous boundary condition (11) remains. The proof is given in Appendix B.

The Green's function can be calculated, for example, by a transfer matrix approach, starting at $z = L$ and ending at $z = 0$. If $\Delta\beta, \kappa^\pm, D_\omega$, and $D_\omega^{\rm gc}$ are set constant within one section of the cavity, (29) can be solved analytically, and the remaining

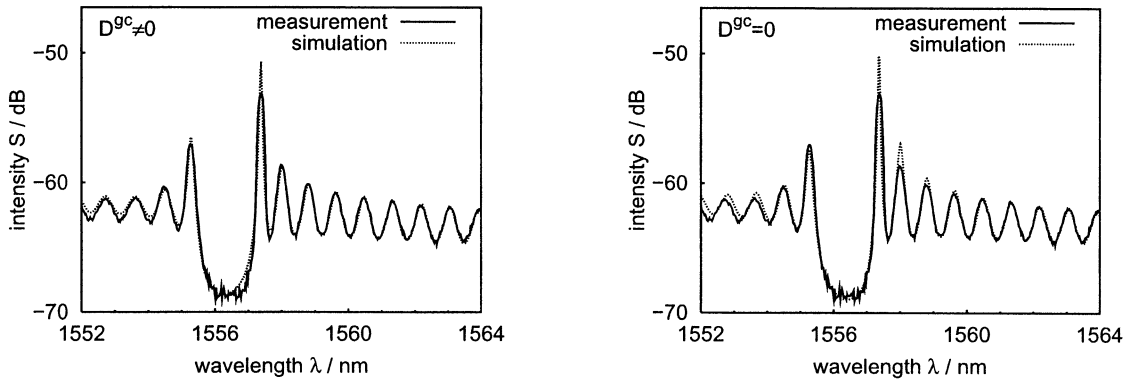

Fig. 1. Measured (solid) and fitted (dashed) ASE spectrum of a truncated-quantum-well DFB laser (a) with interference term and (b) without interference term.

integrals in (28) can be evaluated. The resulting expression for the ASE has to be divided by $|g^{+}_{2,\omega}(0,0) - r_0 g^{-}_{2,\omega}(0,0)|^2$ in order to accomplish the boundary condition (30). For a single-section FP laser, the whole procedure is demonstrated in Appendix C. Note that if the laser threshold $g^{+}_{2,\omega}(0,0) - r_0 g^{-}_{2,\omega}(0,0) = 0$ is approached for some ω, the ASE goes to infinity at this ω.

E. Fitting

The numerical fitting procedure is performed by minimizing the sum of the squared differences between the calculated and the measured spectra values by varying given laser parameters. If N is the number of sampling wavelengths, S_i is the value of the spectrum measured at sampling wavelength λ_i, and $\boldsymbol{p}$ is a vector with the parameters to be determined, then either

$$\sigma^2_{\mathrm{lin}}(\boldsymbol{p}) = \frac{1}{N}\sum_{i=1}^{N}(S(\lambda_i,\boldsymbol{p}) - S_i)^2 \tag{31}$$

or

$$\sigma^2_{\log}(\boldsymbol{p}) = \frac{1}{N}\sum_{i=1}^{N}(\log S(\lambda_i,\boldsymbol{p}) - \log S_i)^2 \tag{32}$$

is minimized by varying the components of $\boldsymbol{p}$. Especially for DFB lasers, the logarithms of the spectra values should be employed in order to attach sufficient importance to the stopband.

The minimization can be performed on the basis of a local or a global numerical search. In contrast to a local search, a global search necessitates no guess values for the parameters to be determined, on the expense of enhanced computational time. Here, we employ a global search using a stochastic derivative-free algorithm, which is combined with a local search [34]. Usually, several minima are found. Among them is hopefully the minimum with the smallest value of $\sigma_{\mathrm{lin}}(\boldsymbol{p})$ or $\sigma_{\log}(\boldsymbol{p})$ corresponding to the best fitted spectrum. In order to perform the minimization, the theoretical model has to be parameterized. The corresponding functions are compiled in Appendix D. The more parameters are known in advance, the better the fitting procedure works and the more reliable the result is.

III. Fitting Results

A. Gain-Coupled DFB Laser

The first example refers to a truncated-quantum-well DFB laser emitting near 1550 nm [35], where we have investigated the influence of D^{gc}_{ω} on the quality of the fit and the parameters to be extracted. Fig. 1 shows the measured spectrum and the best fit taking into account the interference term (a) and neglecting it (b). Both variants allow a good fit of the measured spectrum, although the overall agreement between the measured and the fitted spectrum is slightly better if $D^{\mathrm{gc}}_{\omega} \neq 0$. This is supported by the value of $\sigma_{\log}$, shown in the first row of Table I. The imaginary part of the coupling coefficient κ_i and the gain peak g_p differ strongly between both fitting variants; cf. Table I. Therefore, with previous fitting procedures which set $D^{\mathrm{gc}}_{\omega} = 0$ possibly deviating values of κ_{i} were obtained. Note that the factor $f^{\mathrm{gc}}_{\mathrm{sp}}$ amounts only about one half of f_{sp}.

TABLE I
List of Parameters for Gain-Coupled DFB Laser of Fig. 1. Bold Face: Fitted Results

Parameter	Value	
	$D^{\mathrm{gc}} \neq 0$	$D^{\mathrm{gc}} = 0$
$\sigma_{\log}$	0.117	0.136
R_0	$\mathbf{1.74 \times 10^{-2}}$	$\mathbf{8.92 \times 10^{-3}}$
φ_0	$\mathbf{-0.587}$	$\mathbf{-0.635}$
R_L	0.3	
φ_L	**0.0959**	**0.0955**
L	365 μm	
κ_{r}	**74.8** cm^{-1}	**75.6** cm^{-1}
κ_{i}	**1.38** cm^{-1}	**7.80** cm^{-1}
φ	0	
g_{p}	**14.3** cm^{-1}	**9.17** cm^{-1}
g_{c}	$\mathbf{10^{-4}}$ cm^{-1} nm^{-2}	$\mathbf{10^{-4}}$ cm^{-1} nm^{-2}
λ_0	1555.7 nm	
n_{g}	**3.86**	**3.86**
Δn	$\mathbf{1.70 \times 10^{-3}}$	$\mathbf{1.70 \times 10^{-3}}$
f_{sp}	$\mathbf{1.19 \times 10^{-3}}$	$\mathbf{1.06 \times 10^{-3}}$
$f^{\mathrm{gc}}_{\mathrm{sp}}$	$\mathbf{5.20 \times 10^{-4}}$	0
$\Delta\lambda_{\mathrm{sp}}$	50 nm	
λ_{sp}	1540 nm	

B. Index-Coupled DFB Laser With Second-Order Grating

The next example is a high-power index-coupled DFB laser emitting near 860 nm [36]. It has a second-order grating with a duty cycle >0.5 and a small coupling coefficient $\kappa_r \approx 1$ cm^{-1}. The facets are anti- and high-reflection coated. The measured and the fitted spectrum is depicted in Fig. 2 and the determined parameters are collected in Table II. By virtue of the fit, for the first time we were able to reveal that our antireflection

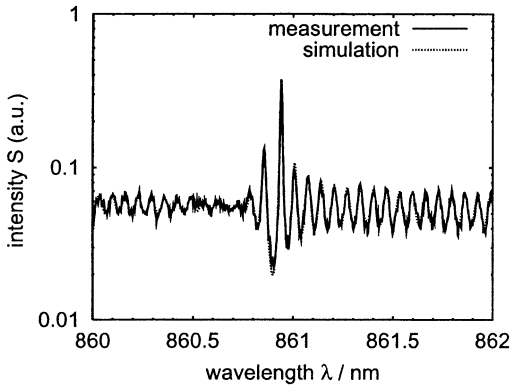

Fig. 2. Measured (solid) and fitted (dashed) ASE spectrum of an index-coupled second-order DFB laser.

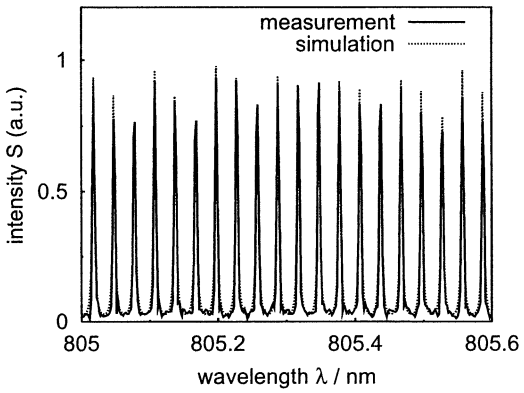

Fig. 3. Measured (solid) and fitted (dotted) ASE spectrum of a tapered FP laser.

TABLE II
LIST OF PARAMETERS FOR SECOND-ORDER DFB LASER OF FIG. 2. BOLD FACE: FITTED RESULTS

Parameter	Value
R_0	$\mathbf{8.78 \times 10^{-5}}$
φ_0	$\mathbf{-0.994}$
R_L	0.95
φ_L	$\mathbf{0.656}$
L	1500 μm
κ_r	$\mathbf{-1.37}$ cm^{-1}
κ_i	$\mathbf{-0.0525}$ cm^{-1}
φ	0
g_p	$\mathbf{15.9}$ cm^{-1}
g_c	0.01 cm^{-1} nm^{-2}
λ_p	855 nm
λ_0	860.9 nm
n_g	$\mathbf{3.79}$
Δn	$\mathbf{9.50 \times 10^{-6}}$
f_{sp}	$\mathbf{9.1 \times 10^{-7}}$
g_{sp}	0
$\Delta\lambda_{sp}$	50 nm
λ_{sp}	855 nm

coating yields reflection coefficients $<10^{-4}$. The value of R_0 obtained by fits of spectra measured at different injection currents below threshold varies between 8 and 9×10^{-5}. For FP lasers, it is difficult to extract the reflection coefficients from the spectra, because according to (C5) the peak-to-valley ratio of the longitudinal modes depends only on the net gain $g - \alpha + (1/L)\ln(\sqrt{R_0 R_L})$.

C. Tapered FP Laser

The last example treats a 2750-μm-long tapered laser consisting of a 750-μm-long index-guided straight section and a 2000-μm-long gain-guided tapered section [37]. Between both sections, there is a waveguide discontinuity that leads to a modulation of the envelope of the spectrum shown in Fig. 3. The reflection coefficient at the discontinuity was fitted to be about $R_d = 10^{-5}$. If we Fourier-transform the spectrum over a larger wavelength range and scale the abscissa properly, we obtain major peaks at multiples of the cavity length. The modulation of the spectrum leads to additional peaks between them. They occur exactly at the positions of the discontinuity (see Fig. 4) measured from either side of the cavity. The Fourier transformed measured spectrum exhibits only one additional peak, the reason

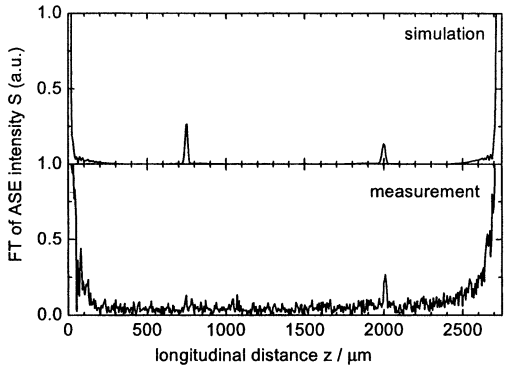

Fig. 4. Fourier transformation of the spectra of Fig. 3 taken between 793 and 811 nm. The abscissa has been scaled in such a way that the position of the second major peak coincides with the total cavity length.

of which is not clear. This method of analyzing ASE spectra of FP lasers can be used for defect recognition [2], [38]–[40].

IV. CONCLUSION

Based on a new method to solve the inhomogeneous coupled wave equations, a new expression for the ASE of multisection lasers is derived. For gain-coupled DFB lasers, and only for that, it contains an additional term due to cross correlation of forward- and backward-propagating spontaneously emitted photons. The theoretical model has been successfully integrated in a parameter extraction program. Due to its simplicity, it can be easily implemented in numerical laser simulators that solve the coupled-wave equations.

APPENDIX A

In this appendix, we prove that (20) is a solution of (4) taking into account (23) and (24). Using the fact that the Green's functions are symmetric with respect to an exchange of their arguments, $\mathrm{G}_{1,\omega}(z,z') = \mathrm{G}_{1,\omega}(z',z)$, and introducing (4) into the first row of (20), we obtain

$$\begin{aligned}\psi_\omega^+(z) &= (\mathrm{G}_{1,\omega}(z',z), \mathbf{H}_\omega(z')\Psi_\omega(z')) \\ &= (\mathbf{H}_\omega(z')\mathrm{G}_{1,\omega}(z',z), \Psi_\omega(z')) \\ &= \left(\begin{bmatrix} 0 \\ \delta(z'-z) \end{bmatrix}, \Psi_\omega(z')\right) \\ &= \psi_\omega^+(z) \end{aligned} \tag{A1}$$

where we exploit the symmetry property (19) of the operator $\mathbf{H}_\omega$ and insert (23). The second row of (20) can be proven similarly.

APPENDIX B

In this appendix, we prove the equivalence of (24) for $z'=0$ and (29) and (30). If we integrate (24) in a small interval $[z'-\epsilon, z'+\epsilon]$ around z', we obtain

$$1 = g_{2\omega}^{+}(z'+\epsilon, z') - g_{2\omega}^{+}(z'-\epsilon, z') \tag{B1}$$

and

$$0 = g_{2\omega}^{-}(z'+\epsilon, z') - g_{2\omega}^{-}(z'-\epsilon, z') \tag{B2}$$

where we omitted all unimportant terms, which vanish if we take the limit $\epsilon \to 0$. If we place the left facet at $z = 0-\epsilon$, we can derive from (B1) at $z'=0$ taking into account (10) and (B2)

$$\begin{aligned} 1 &= g_{2\omega}^{+}(+\epsilon, 0) - g_{2\omega}^{+}(-\epsilon, 0) \\ &= g_{2\omega}^{+}(+\epsilon, 0) - r_0 g_{2\omega}^{-}(-\epsilon, 0) \\ &= g_{2\omega}^{+}(+\epsilon, 0) - r_0 g_{2\omega}^{-}(+\epsilon, 0). \end{aligned} \tag{B3}$$

Hence, in the limit for $\epsilon \to 0$, the Green's function $\mathrm{G}_{2,\omega}(z,0)$ obeys the inhomogeneous boundary condition (30).

APPENDIX C

In this appendix, we derive the ASE spectral density of a single-section FP laser in order to show the equivalence to former expressions. Let us set $g_{2\omega}^{+}(L,0)=1$. Then from (11), $g_{2\omega}^{-}(L,0)=r_L$ follows. The solution of (29) is

$$g_{2\omega}^{+}(z,0) = \mathrm{e}^{-i\Delta\beta(z-L)} \tag{C1}$$

and

$$g_{2\omega}^{-}(z,0) = r_L \mathrm{e}^{+i\Delta\beta(z-L)}. \tag{C2}$$

The integration yields

$$\begin{aligned} \int_0^L &[|g_{2,\omega}^{+}(z,0)|^2 + |g_{2,\omega}^{-}(z,0)|^2]\,dz \\ &= \frac{1}{2\mathrm{Im}\beta L}\left[1 - r_L^2 - \mathrm{e}^{-2\mathrm{Im}\beta L} + r_L^2 \mathrm{e}^{+2\mathrm{Im}\beta L}\right]. \end{aligned} \tag{C3}$$

The integral has to be divided by

$$|g_{\omega}^{+}(0,0) - r_0 g_{\omega}^{-}(0,0)|^2 = \mathrm{e}^{-2\mathrm{Im}\beta L}|1 - r_0 r_L \mathrm{e}^{-2i\Delta\beta L}|^2 \tag{C4}$$

in order to accomplish the boundary condition (30). After some rearrangements, the ASE emerging from the left facet is found to be given by

$$\begin{aligned} &S_{\omega}^{-}(-0) \\ &= \frac{\hbar\omega n_{\mathrm{sp}} g[1-|r_0|^2]\left[\mathrm{e}^{(g-\alpha)L}-1\right]\left[r_L^2\mathrm{e}^{(g-\alpha)L}+1\right]}{(g-\alpha)\left|1 - r_0 r_L \mathrm{e}^{(g-\alpha)L}\mathrm{e}^{-2i\mathrm{Re}(\Delta\beta)L}\right|^2}. \end{aligned} \tag{C5}$$

This expression is equivalent to [9, eq. (64)], except for an unimportant prefactor.

APPENDIX D

In this appendix, the model functions to be used in the fitting procedure are compiled. Instead of frequency ω, the corresponding vacuum wavelength λ is used as a variable.

The amplitude reflection coefficients at the facets are given by

$$\begin{aligned} r_0 &= \sqrt{R_0}\mathrm{e}^{2\pi i\varphi_0} \\ r_L &= \sqrt{R_L}\mathrm{e}^{-2\pi i\varphi_L} \end{aligned} \tag{D1}$$

with the power reflection coefficients R_0 and R_L. Note that the phases φ_0 and φ_L depend on φ. A discontinuity is characterized by its power reflection and transmission coefficients R_d and T_d, as well as a phase φ_d

$$\begin{aligned} r^{+} &= -\sqrt{R_d}\mathrm{e}^{-2\pi i\varphi_d} \\ r^{-} &= -r^{+*} \\ t^{+} &= t^{-} = \sqrt{T_d}. \end{aligned} \tag{D2}$$

The relative propagation coefficient including the radiation loss consists of a real part and an imaginary part proportional to the relative effective index and gain, respectively. The real part is linearized with respect to frequency so that an effective group index n_{g} is introduced. The spectrum of the imaginary part is approximated to be parabolic. Therefore

$$\begin{aligned} &\Delta\beta(z,\lambda) + i\kappa_{\mathrm{i}}^{\mathrm{rad}}(z,\lambda) \\ &\quad = \frac{2\pi}{\lambda_0}\left\{n_{\mathrm{g}}(z)\left[\frac{\lambda_0}{\lambda}-1\right] + \Delta n(z)\right\} \\ &\qquad + \frac{i}{2}\{g_p(z) - g_{\mathrm{c}}(z)[\lambda - \lambda_p(z)]^2\} \end{aligned} \tag{D3}$$

where λ_0 is a reference wavelength, Δn describes an additional index variation, g_p is the peak value of the imaginary part at wavelength λ_p, and g_c is the curvature of its wavelength dependence.

The spectrum of the spontaneous emission is modeled by a Lorentzian with full width $\Delta\lambda_{\mathrm{sp}}$ at half maximum and center wavelength λ_{sp}. Therefore, the diffusion coefficients (16) and (17) are given by

$$D(z,\lambda) = f_{\mathrm{sp}}(z)\frac{\lambda_0}{\lambda}\frac{[\Delta\lambda_{\mathrm{sp}}(z)/2]^2}{[\Delta\lambda_{\mathrm{sp}}(z)]^2 + [\lambda_{\mathrm{sp}}(z)-\lambda]^2} \tag{D4}$$

$$D^{\mathrm{gc}}(z,\lambda) = f_{\mathrm{sp}}^{\mathrm{gc}}(z)\frac{\lambda_0}{\lambda}\frac{[\Delta\lambda_{\mathrm{sp}}(z)/2]^2}{[\Delta\lambda_{\mathrm{sp}}/2(z)]^2 + [\lambda_{\mathrm{sp}}(z)-\lambda]^2}\mathrm{e}^{-2\pi i\varphi} \tag{D5}$$

where f_{sp} and $f_{\mathrm{sp}}^{\mathrm{gc}}$ govern the strength of the spontaneous emission.

ACKNOWLEDGMENT

The author would like to thank J. Kreissl, HHI Berlin, for providing the experimental data of the gain-coupled DFB laser and A. Klehr, FBH Berlin, for the measurements of the spectra of the index-coupled second-order DFB laser and the tapered FP laser.

REFERENCES

[1] B. Hakki and T. Paoli, "Gain spectra in GaAs double-heterostructure injection lasers," *J. Appl. Phys.*, vol. 46, pp. 1299–1306, Mar. 1975.

[2] L. F. D. Chiaro, "Damage-induced spectral perturbations in multilongitudinal-mode semiconductor lasers," *J. Lightwave Technol.*, vol. 8, pp. 1659–1669, Nov. 1990.

[3] H. Soda and H. Imai, "Analysis of the spectrum behavior below the threshold in DFB lasers," *IEEE J. Quantum Electron.*, vol. 22, pp. 637–641, May 1986.

[4] T. Makino and J. Glinski, "Transfer matrix analysis of the amplified spontaneous emission of DFB semiconductor laser amplifiers," *IEEE J. Quantum Electron.*, vol. 24, pp. 1507–1518, Aug. 1988.
[5] S. Hansmann, "Transfer matrix analysis of the spectral properties of complex distributed feedback laser structures," *IEEE J. Quantum Electron.*, vol. 28, pp. 2589–2595, Nov. 1992.
[6] G. Morthier, K. Sato, R. Baets, T. K. Sudoh, Y. Nakano, and K. Tada, "Parameter extraction from subthreshold spectra in cleaved gain- and index coupled DFB LDs," in *Tech. Dig. OFC'95*, Mar. 1995, pp. 309–310.
[7] T. Nakura and Y. Nakano, "LAPAREX—An automatic parameter extraction program for gain- and index-coupled distributed feedback semiconductor lasers, and its application to observation of changing coupling coefficient with currents," *IEICE Trans. Electron.*, vol. E83-C, pp. 488–495, Mar. 2000.
[8] G. B. Morrison and D. Cassidy, "A probability-amplitude transfer matrix model for distributed-feedback laser structures," *IEEE J. Quantum Electron.*, vol. 36, pp. 633–640, June 2000.
[9] C. Henry, "Theory of spontaneous emission noise in open resonators and its application to lasers and optical amplifiers," *J. Lightwave Technol.*, vol. 4, pp. 288–297, Mar. 1986.
[10] T. Makino, "Transfer-matrix formulation of spontaneous emission noise of DFB semiconductor lasers," *J. Lightwave Technol.*, vol. 9, pp. 84–91, Jan. 1991.
[11] G.-H. Duan, "Generalized noise analysis of spatially inhomogeneous laser amplifiers," *Opt. Lett.*, vol. 18, pp. 275–277, Feb. 1993.
[12] T. Makino, "Amplified spontaneous emission model for quantum-well distributed feedback lasers," *IEEE J. Quantum Electron.*, vol. 33, pp. 1010–1017, June 1997.
[13] R. Schatz, E. Berglind, and L. Gillner, "Parameter extraction from DFB lasers by means of a simple expression for the spontaneous emission spectrum," *IEEE Photon. Technol. Lett.*, vol. 6, pp. 1182–1184, Oct. 1994.
[14] J.-P. Weber and S. Wang, "A new method for the calculation of the emission spectrum of DFB and DBR lasers," *IEEE J. Quantum Electron.*, vol. 27, pp. 2256–2266, Oct. 1991.
[15] E. Berglind and L. Gillner, "Optical quantum noise tread with classical electrical network theory," *IEEE J. Quantum Electron.*, vol. 30, pp. 846–853, Mar. 1994.
[16] W. Fang, A. Hsu, S. L. Chuang, T. Tanbun-Ek, and A. M. Sergent, "Measurement and modeling of distributed-feedback lasers with spatial hole-burning," *IEEE J. Select. Topics Quantum Electron.*, vol. 3, pp. 547–554, Apr. 1997.
[17] U. Bandelow and U. Leonhardt, "Light propagation in one-dimensional lossless dielectrica: Transfer matrix method and coupled mode theory," *Opt. Commun.*, vol. 101, pp. 92–99, Aug. 1993.
[18] H.-J. Wünsche, U. Bandelow, and H. Wenzel, "Calculation of combined lateral and longitudinal in $\lambda/4$ shifted DFB lasers," *IEEE J. Quantum Electron.*, vol. 29, pp. 1751–1760, June 1993.
[19] J. Skagerlund, F. Pusa, O. Sahlen, L. Gillner, R. Schatz, P. Granestrand, L. Lundqvist, B. Stoltz, J. Terlecki, F. Wahlin, A.-C. Mörner, J. Wallin, and O. Öberg, "Evaluation of an automatic method to extract the grating coupling coefficient in different types of fabricated DFB lasers," *IEEE J. Quantum Electron.*, vol. 34, pp. 141–146, Jan. 1998.
[20] G. M. D. Cassidy and D. M. Bruce, "Facet phases and sub-threshold spectra of DFB lasers: Spectral extraction, features, explanations, and verification," *IEEE J. Quantum Electron.*, vol. 37, pp. 762–769, June 2001.
[21] LASFIT—A laser diode parameter extractor [Online]. Available: http://www.photond.com/products/lasfit/lasfit.htm
[22] LAPAREX—A laser parameter extraction program [Online]. Available: http://www.ee.t.u-tokyo.ac.jp/~nakano/lab/LAPAREX/
[23] G. Morrison and D. Cassidy, "A probability-amplitude transfer-matrix method for calculating the distribution of light in semiconductor lasers," *IEEE J. Quantum Electron.*, vol. 39, pp. 431–437, Mar. 2003.
[24] B. Tromborg, H. Lassen, and H. Olesen, "Traveling wave analysis of semiconductor lasers: Modulation response, mode stability, and quantum mechanical treatment of noise spectra," *IEEE J. Quantum Electron.*, vol. 1994, pp. 939–956, Apr. 1994.
[25] F. Randone and I. Montrosset, "Analysis and simulation of gain-coupled distributed feedback semiconductor lasers," *IEEE J. Quantum Electron.*, vol. 31, pp. 1964–1973, Nov. 1995.
[26] G. Morthier, R. Baets, A. Tsigopoulos, T. Sphicopoulos, F. Tsang, J. E. Carrol, H. Wenzel, A. Mecozzi, A. Sapia, P. Correc, S. Hansmann, H. Burkhard, A. Paradisi, I. Montrosset, H. Olesen, E. E. Lassen, R. Schatz, and H. Bissesur, "Comparison of different DFB laser models within the European COST 240 collaboration," *Proc. Inst. Elect. Eng. J. Optoelectron.*, vol. 141, pp. 82–88, 1994.
[27] R. G. Baets, K. David, and G. Morthier, "On the distinctive features of gain coupled DFB lasers and DFB lasers with second-order grating," *IEEE J. Quantum Electron.*, vol. 29, pp. 1792–1798, June 1993.
[28] A. Shams-Zadeh-Amiri, J. Hong, X. Li, and W.-P. Huang, "Second and higher order resonant gratings with gain or loss—Part I: Green's function analysis," *IEEE J. Quantum Electron.*, vol. 36, pp. 1421–1430, Dec. 2000.
[29] H. Olesen, B. Tromborg, X. Pan, and H. Lassen, "Stability and dynamic properties of multi-electrode laser diodes using a Green's function approach," *IEEE J. Quantum Electron.*, vol. 1993, pp. 2282–2301, Aug. 1993.
[30] H. Wenzel and H.-J. Wünsche, "An equation for the amplitudes of the modes in semiconductor lasers," *IEEE J. Quantum Electron.*, vol. 30, pp. 2073–2080, Sept. 1994.
[31] H. Wenzel, U. Bandelow, H.-J. Wünsche, and J. Rehberg, "Mechanisms of fast self pulsations in two-section DFB lasers," *IEEE J. Quantum Electron.*, vol. 32, pp. 69–78, Jan. 1996.
[32] C. Henry, "Phase noise in semiconductor lasers," *J. Lightwave Technol.*, vol. 4, pp. 298–311, Mar. 1986.
[33] M. Pereira, Jr. and K. Henneberger, "Green's function theory for semiconductor-quantum-well laser spectra," *Phys. Rev. B*, vol. 53, pp. 16 485–16 496, June 1996.
[34] Optimization Package GLOBAL by Tibor Csendes [Online]. Available: http://users.bigpond.net.au/amiller/
[35] J. Kreissl, private communication.
[36] H. Wenzel, M. Braun, G. Erbert, and G. Tränkle, "High-power DFB lasers," in *Tech. Dig. CLEO 2002*, May 2002, p. 596.
[37] B. Sumpf, R. Hülsewede, G. Erbert, C. Dzionk, J. Fricke, A. Knauer, W. Pittroff, P. Ressel, J. Sebastian, H. Wenzel, and G. Tränkle, "High-brightness 735 nm tapered diode lasers," *Electron. Lett.*, vol. 38, pp. 183–184, Feb. 2002.
[38] B. D. Patterson, J. E. Epler, B. Graf, H. W. Lehmann, and H. C. Sigg, "A superluminescent diode at 1.3 μm with very low spectral modulation," *IEEE J. Quantum Electron.*, vol. 30, pp. 703–711, Mar. 1994.
[39] D. Hofstetter and R. L. Thornton, "Measurement of optical cavity properties in semiconductor lasers by Fourier analysis of the emission spectrum," *IEEE J. Quantum Electron.*, vol. 34, pp. 1914–1923, Oct. 1998.
[40] A. Klehr, G. Beister, G. Erbert, A. Klein, J. Maege, I. Rechenberg, J. Sebastian, H. Wenzel, and G. Tränkle, "Defect recognition via longitudinal mode analysis of high power fundamental mode and broad area edge emitting laser diodes," *J. Appl. Phys.*, vol. 90, pp. 43–47, July 2001.

Hans Wenzel received the Dipl. and Ph.D. degrees in physics from Humboldt-University, Berlin, Germany, in 1986 and 1991, respectively. His thesis dealt with the electrooptical modeling of semiconductor lasers.

From 1991 to 1994, he was involved in a research project on the three-dimensional simulation of DFB lasers. In 1994, he joined the Ferdinand-Braun-Institut für Höchstfrequenztechnik, Berlin, Germany, were he is engaged in the development of high-power semiconductor lasers. His main research interests include the analysis, modeling, and simulation of optoelectronic devices.